

A fluorometric paper-based sensor array for the discrimination of volatile organic compounds (VOCs) with novel salicylidene derivatives



Thiti Jarangdet^{a,b}, Kornkanya Pratumyot^a, Kittiwat Srikittiwanna^a, Wijitar Dungchai^a,
Withawat Mingvanish^a, Ittipon Techakriengkrai^c, Mongkol Sukwattanasinitt^d,
Nakorn Niamnont^{a,b,*}

^a Organic Synthesis, Electrochemistry & Natural Product Research Unit, Department of Chemistry, Faculty of Science, King Mongkut's University of Technology Thonburi, Bangkok, 10140, Thailand

^b Luminescence & Scintillation Materials Research Unit, Faculty of Science, King Mongkut's University of Technology Thonburi, Bangkok, 10140, Thailand

^c Department of Food Technology, Faculty of Science, Ramkhamhaeng University, Bangkok 10240, Thailand

^d Department of Chemistry, Faculty of Science and Nanotec-CU Center of Excellence on Food and Agriculture, Chulalongkorn University, Bangkok, 10330, Thailand

ABSTRACT

In this paper, novel salicylidene fluorescent sensors (**1**, **2**, and **3**) were successfully synthesized by the one pot condensation reaction and coated onto filter paper to produce fluorometric paper-based sensor array. The compound **1**, **2**, and **3** paper-based sensor arrays exhibited rapid fluorescent signal in response to exposure to 15 different VOC vapors. A smartphone was used as an alternative device to monitor the appearance of fluorescent signals. The images photographed using the smartphone camera were analyzed for RGB values by a conventional image-processing program. The Δ RGB data set (3 fluorophores \times 15 VOC vapors \times 4 repeats) from fluorescent images of 15 VOC vapors analysis have been statistically categorized by using principal component analysis (PCA) into 15 clusters with 100% discriminating accuracy. The proposed sensor array showed high potential as a portable electronic nose (e-nose) system for VOC vapors discrimination.

1. Introduction

Volatile organic compounds (VOCs) are either subtracted from inspired air (by degradation and/or excretion in the body) or added to alveolar breath as products of metabolism [1]. They do not include carbon monoxide, carbon dioxide, carbonic acid, metallic carbides or carbonates and ammonium carbonate [2]. They are found everywhere both in indoor and outdoor environments because they are essential ingredients in many products and materials. Consequently, VOCs may have short- and long-term adverse health effects on humans, e.g. nervous system impairment, asthma and cancer [3]. The measurement of VOCs level both in indoor and outdoor environments has been important and may be applicable to simply diagnose some acute and chronic diseases such as lung cancer from analysis of a patient's breath [4a,4b]. Nowadays, many efforts have been made to actively develop techniques for detecting and identifying volatile organic compounds (VOCs) in indoor and outdoor environments and in acute and chronic disease diagnostics [5a–d]. In order to determine VOCs at very low levels of concentration, there is high necessity/need for the

development of highly sensitive and selective devices [5a–d]. Although the detection of very small amounts of VOCs can be achieved by using standard analytical techniques [6] such as GC or GC-MS, these techniques require specialists to operate and take long time to analyze are expensive and cannot be portable [7a,7b]. Therefore, simple, rapid and economic devices which can on-site analyze VOCs are highly demanded. As a result, a portable electronic nose (e-nose) system based on mobile sensors has been prevalently designed and developed [8a,8b]. The electrochemical [(5a)], color [9a–e], and fluorescent modes [10a–e] applied for the VOCs detection and identification of sensor array have been continually reported [11]. However, their applications are still limited only to identify amine compounds, and are applied to more number of sensors to discriminate VOCs [12a–f]. A real need for the development of high-performance portable VOC sensor arrays therefore still remains. Fluorescent technique has more advantages due to its high sensitivity and selectivity, more safety, high-throughput analysis, low cost, enabling portability, and simplicity to end-users [13a,13b].

Salicylidene fluorophores containing benzene, nitrophenol,

* Corresponding author. Organic Synthesis, Electrochemistry & Natural Product Research Unit, Department of Chemistry, Faculty of Science, King Mongkut's University of Technology Thonburi, Bangkok, 10140, Thailand.

E-mail address: nakorn.nia@kmutt.ac.th (N. Niamnont).

<https://doi.org/10.1016/j.dyepig.2018.06.044>

Received 28 April 2018; Received in revised form 24 June 2018; Accepted 25 June 2018

Available online 30 June 2018

0143-7208/© 2018 Elsevier Ltd. All rights reserved.

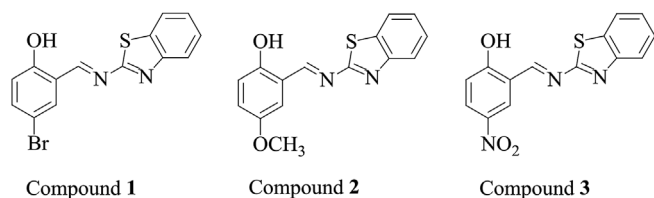


Fig. 1. Structures of benzothiazole-salicylidene derivatives 1, 2, and 3.

naphthalene, pyrene and bisphenol A have been reported to give high sensitivity and selectivity via an excited state intramolecular proton transfer (ESIPT) process and a Schiff base process towards fluoride detection [14a–f]. However, most salicylidene derivatives have not been studied to be the fluorescent paper-based sensor arrays for VOC vapors detection. In this work, we reported the effectiveness of the fluorescent paper-based sensor arrays embedded with novel benzothiazole-salicylidene derivatives for detecting VOCs. The sensor arrays generate different fluorescent signal profiles as exposed to VOC analysts, which lead to the detection and qualitative recognition of the 15 different VOC vapors. Novel benzothiazole-salicylidene fluorophores used for fluorescent paper-based sensor arrays for VOCs were shown in Fig. 1. Numerical data of fluorescent signals to VOC vapors were conveniently collected by a smartphone in the form of images and further analyzed by principal component analysis (PCA) program to identify 15 VOC vapors.

2. Experimental

2.1. Reagents and apparatus

2-Hydroxy-5-methoxybenzaldehyde, 5-nitrosalicylaldehyde, 5-bromosalicylaldehyde, 2-aminobenzothiazole were purchased from Tokyo Chemical Industry (TCI). All other reagents were non-selectively purchased from Sigma-Aldrich, Fluka, Merck or RCI Labscan and used without further purification. Generally, solvents such as acetonitrile, dichloromethane and ethanol were reagent grade and were stored over 4 Å molecular sieves before use. All reactions were carried out under N₂ atmosphere. Additionally, silica gel 60 F254 thin layer chromatography (TLC) was used for following the progress of a reaction.

2.2. Analytical instrument

The ¹H and ¹³C NMR spectra were performed for benzothiazole-salicylidene derivatives 1, 2, and 3 on a Bruker Avance Spectrometer (400 MHz, 100 MHz for ¹H and ¹³C) using tetramethylsilane as the internal standard. The number of absorption signals in the ¹H NMR spectra was designated as follows: s/singlet; d/doublet, t/triplet, dd/double doublet, q/quartet, m/multiplet. Infrared spectra was performed with a Thermo fisher scientific instrument (model Nicolet 8700) using KBr pellets. High resolution electrospray ionization mass spectra (HRMS) were acquired on a Bruker maXis using acetonitrile as a solvent in the positive ionization mode. Melting points were measured using a Thomas Hoover capillary instrument and their values were not subsequently corrected. Fluorescent spectra were measured on a Hitachi F-2500 fluorescence spectrophotometer. UV-Vis absorption spectra were measured on a Perkin Elmer Ltd, lambda 35/fias 300 UV-vis spectrophotometer. Fluorescent intensity in multisampling was recorded on EnSpire multimode plate reader, Perkin-Elmer.

2.3. Synthesis of compound 1

5-bromosalicylaldehyde (200 mg, 0.995 mmol), 2-aminobenzothiazole (165 mg, 1.1 mmol) and ethanol (5 mL) were introduced into a sealed tube (100 mL) under N₂ atmosphere and the reaction mixture was stirred for 3 h at 78 °C. After the reaction mixture was cooled

down, the precipitated solid was filtered off and washed with cool ethanol (3 × 15 mL) which was purified by recrystallization with ethanol. Compound 1 was obtained as an orange crystal (205 mg, 62% yield), mp: 188–190 °C; δ_H (400 MHz, CDCl₃) 12.24 (1H, s), 9.22 (1H, s), 7.99 (2H, d, *J* = 8.0 Hz), 7.86 (4H, d, *J* = 8 Hz), 7.64 (1H, d, *J* = 2.4 Hz), 7.56–7.48 (1H, m), 7.41 (1H, t, *J* = 8.0 Hz), 6.98 (1H, d, *J* = 12.0 Hz); δ_C (100 MHz, CDCl₃) 168.4, 166.0, 160.9, 151.5, 137.9, 135.7, 134.8, 126.9, 125.5, 123.3, 121.8, 119.7, 111.3; HRMS-ESI *m/z* calcd for C₁₄H₉BrN₂OS: 334.9677 [M+H]⁺, Found: 334.9742 [M+H]⁺.

2.4. Synthesis of compound 2

2-Hydroxy-5-methoxybenzaldehyde (200 mg, 1.31 mmol), 2-aminobenzothiazole (210 mg, 1.40 mmol) and ethanol (5 mL) were introduced into a sealed tube (100 mL) under N₂ atmosphere and the reaction mixture was stirred for 3 h at 78 °C. After the reaction mixture was cooled down and the precipitated solid was filtered off and washed with cool ethanol (3 × 15 mL) which was purified by recrystallization with ethanol. Compound 2 was obtained as a red crystal (268 mg, 72% yield), mp: 144–146.5 °C; δ_H (400 MHz, CDCl₃) 11.86 (1H, s), 9.25 (1H, s), 7.97 (1H, d, *J* = 8.0 Hz), 7.85 (1H, d, *J* = 8.0 Hz), 7.50 (1H, td, *J* = 1.2, 8.4 Hz), 7.39 (1H, td, *J* = 1.2, 8.4 Hz), 7.11 (1H, dd, *J* = 4.0, 8.0 Hz), 7.05–6.95 (2H, m), 3.02 (3H, s). δ_C (100 MHz, CDCl₃) 169.1, 167.1, 156.6, 152.6, 151.5, 134.7, 126.7, 125.3, 123.7, 123.0, 121.8, 118.7, 117.8, 115.7, 115.2, 55.9; HRMS-ESI *m/z* calcd for C₁₅H₁₂N₂O₂S: 285.0692 [M+H]⁺, Found: 285.0778 [M+H]⁺.

2.5. Synthesis of compound 3

5-nitrosalicylaldehyde (200 mg, 1.20 mmol), 2-aminobenzothiazole (210 mg, 1.4 mmol) and ethanol (5 mL) were introduced into a sealed tube (100 mL) under N₂ atmosphere and the reaction mixture was stirred for 3 h at 78 °C. After the reaction mixture was cooled down, the precipitated solid was filtered off and washed with cool ethanol (3 × 15 mL) which was purified by recrystallization with ethanol. Compound 3 was obtained as a red crystal (301 mg, 84% yield), mp: 231–233 °C; δ_H (400 MHz, CDCl₃) 13.10 (1H, s), 9.40 (1H, s), 8.53 (1H, d, *J* = 4 Hz), 8.36 (1H, dd, *J* = 4, 8 Hz), 8.02 (1H, d, *J* = 8 Hz), 7.89 (1H, d, *J* = 8 Hz), 7.55 (1H, t, *J* = 8 Hz), 7.44 (1H, t, *J* = 8 Hz), 7.17 (1H, d, *J* = 8 Hz). δ_C (100 MHz, CDCl₃) 195.4, 166.6, 165.5, 131.7, 129.9, 129.7, 127.1, 125.9, 123.6, 121.9, 119.0, 118.7, 117.6, 77.0; HRMS-ESI *m/z* calcd for C₁₄H₉N₃O₃S: 300.0437 [M+H]⁺, Found: 300.0522 [M+H]⁺.

2.6. Photo-physical property of compounds 1, 2, and 3

The stock solutions of compounds 1, 2, and 3 (500 μM) were prepared in methanol. 100 μM quinine sulfate in 0.05 M H₂SO₄ was used as a standard fluorophore. The UV-Vis absorption spectra between 250 nm to 600 nm were measured using a 1 cm quartz cell at room temperature. The fluorescent spectra of compounds 1, 2, and 3 and quinine sulfate were obtained under light irradiation of 380 nm, 410 nm, 310 nm and 345 nm, respectively. The fluorescence quantum yields of compounds 1, 2, and 3 were calculated by comparing to standard quinine sulfate (*Φ* = 0.54) in 0.1 M H₂SO₄ [15].

2.7. Fabrication of compound 1, 2, and 3 coated papers

The black circle ring for loading sample (5.0 mm of inner diameter) were printed on Whatman filter paper No.1 by HP LaserJet Pro P1102w Printer, and it was coated with the 3M adhesive tape on the backside. Afterwards, 2 μL of the sensory solutions of compounds 1, 2, and 3 in acetone (1 mM) were individually dropped to the filter papers directly [16]. The fabricated papers were then dried using hair drier [12(c)].

2.8. Detection of VOCs and fluorometric measurements

Each VOC (10 mL) was individually added into a TLC developing chamber with a lid (25 mL), and allowed it to reach equilibrium for 60 min. After that, the VOC saturated chamber was covered with the lid having the paper coated with the sensor molecule inside for 5 min at room temperature. The photographic images of the sensory paper saturated with VOC vapor were then recorded under the UV light of 365 nm using i-phone SE with Shutter application of the highest ISO and medium white balance modes. Each image was converted to TIF format file and cropped into a circle of 0.065 cm² areas. The RGB values of the cropped images were analyzed by Image J program. The ΔR , ΔG and ΔB values were obtained from a comparison of the RGB values before and after exposure to VOC saturated vapors. The raw 540 RGB numerical data (3 RGB values \times 15 solvents \times 3 sensors \times 4 repeats) were analyzed by Principal Component Analysis (PCA) was performed by Unscrambler v. 9.7 (CAMO A/S, Oslo, Norway) using full cross validation method. All variables were setting at 1.0/standard deviations for their weights.

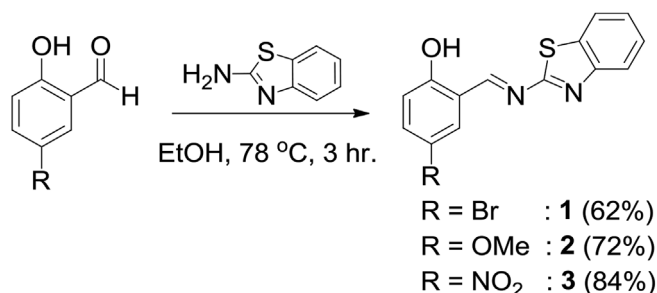
3. Results and discussion

3.1. Synthesis of salicylidene derivatives (1, 2, and 3)

A series of salicylidene derivatives (**1**, **2**, and **3**) were synthesized via the one-step condensation reaction of salicylaldehyde derivatives and 2-aminobenzothiazole with high yield (62–84%) [17]. Indeed, the reaction of 2-aminobenzothiazole with various salicylaldehyde can be considered as one of the green chemistry process due to the utilization of ethanol solvent possessing little or no toxicity to the human health and environment (Scheme 1) [18]. The chemical structures of compounds **1**, **2**, and **3** have been confirmed by ¹H NMR, ¹³C NMR and FT-IR techniques as shown in supporting information (Fig S1–S9). Obviously, ¹H NMR spectra showed the characteristic imine proton signals of compounds **1**, **2**, and **3** at 9.30, 9.30 and 9.40 ppm, respectively. In addition, the presence of the HRMS-ESI molecular ion peaks [M+H]⁺ of compounds **1**, **2**, and **3** at *m/z* 334.9742, 285.0778 and 300.0522, respectively, corresponded to the proposed molecular structures as shown in supporting information (Fig. S10–S12).

3.2. Photo physical properties of compound 1, 2, and 3

The photo-physical properties of compounds **1**, **2**, and **3** are summarized in Table 1. The UV–Vis absorption spectrum of each compound in methanol displayed the maximum absorption wavelength (λ_{\max}) ranging from 310 to 410 nm with two major absorption bands corresponding to the $\pi-\pi^*$ and $n-\pi^*$ transitions. The maximum emission wavelength of each compound was observed in the range between 460 and 560 nm (Fig. S13–S15). The absorption and emission spectra of compounds **1** and **2** exhibited remarkable red-shift phenomenon in comparison with those of compound **3**. This could be explained by the effect of electron withdrawing nitro ($-\text{NO}_2$) group on the



Scheme 1. Synthetic route to compounds **1**, **2**, and **3**.

Table 1

Photo-physical properties of compounds **1**, **2**, and **3** in methanol Solution.

Compounds	λ_{abs} (nm)	$\log \epsilon$	λ_{em} (nm)	Φ
1	270, 380	4.05, 3.29	550	0.0069
2	270, 410	3.93, 3.60	560	0.0855
3	270, 310	4.13, 3.90	540	0.0008

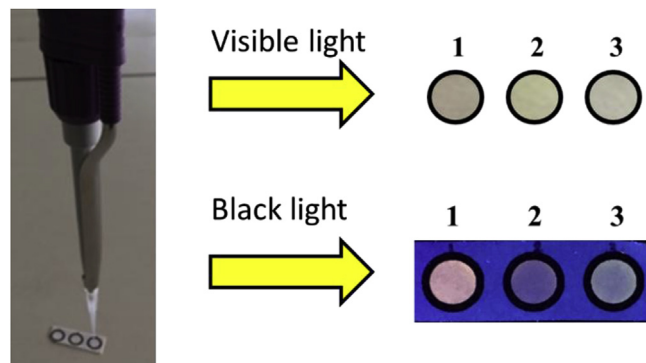


Figure 2. Preparation of paper-based salicylidene sensors.

decrease in the extent of π conjugated system. The fluorescent quantum yields of all compounds were very weak in methanol media, especially that for compound **3**. We expected that the electron-withdrawing nitro group enhanced the excited state intramolecular proton transfer (ESIPT) process in protic solvents [19a,19b], resulting in low fluorescent quantum yields of compound **3** in methanol.

3.3. Preparation of compound 1, 2, and 3 coated papers

Compounds **1**, **2**, and **3** were successfully coated on filter papers with the simple process stated previously (Fig. 2). On the exposure of VOCs vapor, the fabricated paper coated with compounds **1**, **2**, and **3** exhibited fluorescent emission that can be observed by naked eye under UV light at 365 nm. Compounds **1**, **2**, and **3** fabricated on the papers were stable upon storage at least four weeks in the dark at room temperature when exposed to the UV light of 365 nm.

3.4. Fluorescence responses of compounds 1, 2, and 3 to VOCs

Earlier research mainly focused on luminescent properties of salicylidene derivatives towards volatile solvents in liquid phase [20]. However, the best of our knowledge, there is no published paper reporting their detection of VOCs in gaseous phase. Therefore, the compound **1**, **2**, and **3** coated papers were prepared and tested against a wide range of VOCs vapor, i.e. hexane, toluene, benzene, diethyl ether, dichloromethane (CH_2Cl_2), chloroform (CHCl_3), tetrahydrofuran (THF), ethyl acetate (EtOAc) acetone, acetonitrile (MeCN), dimethylformamide (DMF), dimethylsulfoxide (DMSO), 2-propanol, ethanol (EtOH) and methanol (MeOH). Upon exposure to UV light at 365 nm for 5 min, the spots of compounds **1**, **2**, and **3** coated on the paper exhibited a difference in fluorescent emission responses, which was attributed to the different interactions of the sensing compounds with the VOCs tested (Fig. 3). Specifically, the enol-imine group in compounds **1**, **2**, and **3** form intramolecular (O–H) hydrogen bond, which is highly sensitive to local polarity and local hydrogen bond to their oxygen atoms. In polar protic solvents such as methanol, the enol ($-\text{OH}$) group of compounds **1**, **2**, or **3** formed double intermolecular hydrogen bonds with the hydroxyl ($-\text{OH}$) group of methanol and caused the enol-imine group to tautomerize into the keto-enamine group (Scheme 1S in supplementary data) [21]. The excited state intramolecular proton transfer (ESIPT) process that was accounted for this tautomerization was

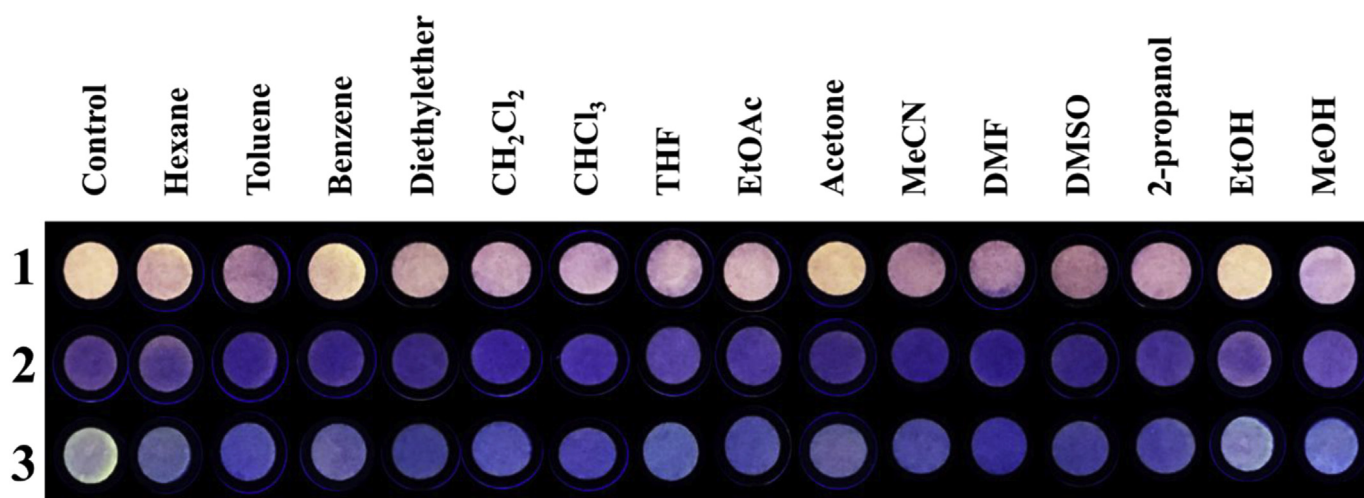


Fig. 3. Fluorescent images of Compound 1, 2, and 3 based paper sensory arrays exposed by various vapors of volatile organic solvents under black light of 365 nm.

responsible for the decrease in fluorescent intensity on exposure of the compound 1, 2, and 3 coated on papers to methanol and ethanol (see Fig. S17(a)-S19(c) in supplementary data) [22]. On the contrary, there was lower ESIPT generated in polar aprotic solvents by hydrogen bond with other solvents, thus the fluorescent intensity of the sensing papers were maintained upon contact with these solvents. In addition, the hydrophobic interaction (London) of compounds 1, 2, and 3 with non-polar solvents helped to stabilize the monomeric form of compounds 1, 2, and 3 from aggregation that caused their fluorescent emission to be quenched. Therefore, the fluorescent intensity of the sensor spots in contact with all VOCs except polar protic ethanol and methanol were still strong emission.

3.5. Evaluation of fluorescent response patterns of compounds 1, 2 and 3 to VOCs

The 45 fluorescent responses of 3 sensors with 15 VOC vapors were transformed into images of TIF type with a digital camera, and then the color of the TIF images was determined and reported to the RGB values (R = red, G = green and B = blue) using ImageJ software program. The three-dimensional vectors (ΔR , ΔG , ΔB) of each salicylidene spot on the image were calculated its RGB values before and after exposure to the VOC vapors. Histogram plot (Fig. 4) shows the changes in ΔR , ΔG , and ΔB values of the three sensors upon exposure to various VOC vapors. Notably, most of the samples exhibited considerable change in the red (R) and green (G) values as compared to the blue (B) values. The images of compound 1 and 3 spots have decreased red and green values, resulting in the negative values of ΔR and ΔG . Additionally, the decrease in the R, G, and B values of compound 3 spots are more dramatic than that of compound 1 spots for most VOCs except methanol and ethanol. The images of compound 2 spots, in contrast, have increased R, G, and B values, leading to the positive values of ΔR , ΔG , and ΔB . These responses were possibly due to the substituent effects that stabilize or destabilize tautomeric form of compounds 1, 2, and 3 over another. The electron donating $-\text{OCH}_3$ group in compound 2 stabilizes the enol-imine tautomeric form by strengthening the O–H bond of the enol, thus reduces the ESIPT and consequently promotes the increased fluorescent signal intensity [23]. On the other hand, the electron withdrawing $-\text{Br}$ and $-\text{NO}_2$ groups in compounds 1 and 3 respectively destabilizes the enol-imine form by weakening the O–H bond of the enol [14(e)], driving the tautomerization toward keto-enamine form. During the tautomerization, the ESIPT process is responsible for the decrease in fluorescent signal intensities. On comparison of the ΔRGB patterns among 15 VOCs, it showed that the non polar solvents, i.e. hexane, toluene and benzene exhibited a subtle change in ΔRGB

patterns, while the polar solvents display a large change in ΔRGB patterns with a remarked change in ΔR values. In particular, the polar protic solvents, i.e. methanol and ethanol displayed the most unique ΔRGB patterns on the sensor arrays that allows them to be distinguished from other VOCs. Therefore, the paper-based sensor arrays of compounds 1, 2, and 3 could selectively detect and identify the presence of methanol and ethanol as compared with other VOCs. The standard deviation as depicted by the error bars in Fig. 4, was calculated from 12 measurements (3 sensors \times 4 repeats), was small which demonstrates the precision of this method of measurement.

3.6. Multivariate statistical analyses of the fluorescent responses of compounds 1, 2 and 3 to VOCs

Variability in fluorescence response patterns can be used to discriminate different compounds. To organize an enormous data set with many variables (15 VOCs \times 3 sensors \times 4 repeats \times 3 values of RGB), the principal analysis (PCA) is an alternative tool to reduce dimensionality of multivariate data by grouping similar observations together. PCA is a statistical multivariate analysis to generate principal component (PC) scores as a data set. Fig. 5 showed that PC1 and PC2 were taken into account for 52% and 25% of the data variance, respectively. The 2D PCA plot clearly shows the high discriminating ability of the compound 1, 2, and 3 paper-based sensor array towards 15 VOCs. As expected, methanol, which showed the unique ΔRGB pattern among other VOCs, had the highest PC1 and PC2 scores. To evaluate the classification accuracy, factorial discriminant analysis (FDA) was applied on the PC scores to cross validate the discriminating ability using a leave-one-out technique [24]. The FDA cross validation gave 100% classification accuracy. The results emphasized the high effectiveness of the novel salicylidene derivatives 1, 2, and 3 applied on a fluorometric paper-based sensor array for detection and identification of VOCs.

Due to the most distinguishable PC score of methanol, the compound 1, 2, and 3 paper-based sensor array have been selected for testing the real methanol samples. In order to gather more details of the methanol detection, we have set out to test the effect of concentration of methanol on color change of the compound 3 spot on paper-based sensor array. The compound 3 spot was used in this experiment because it showed the most obvious color change upon contact with methanol as compared with compounds 1 and 2. To investigate the fluorescent behavior of compound 3 towards methanol concentration, a paper-based sensor array of compound 3 spots was exposed to 6 different concentrations of methanol solution in water. Upon exposure to methanol vapors in water for 5 min, the compound 3 paper-based sensor array

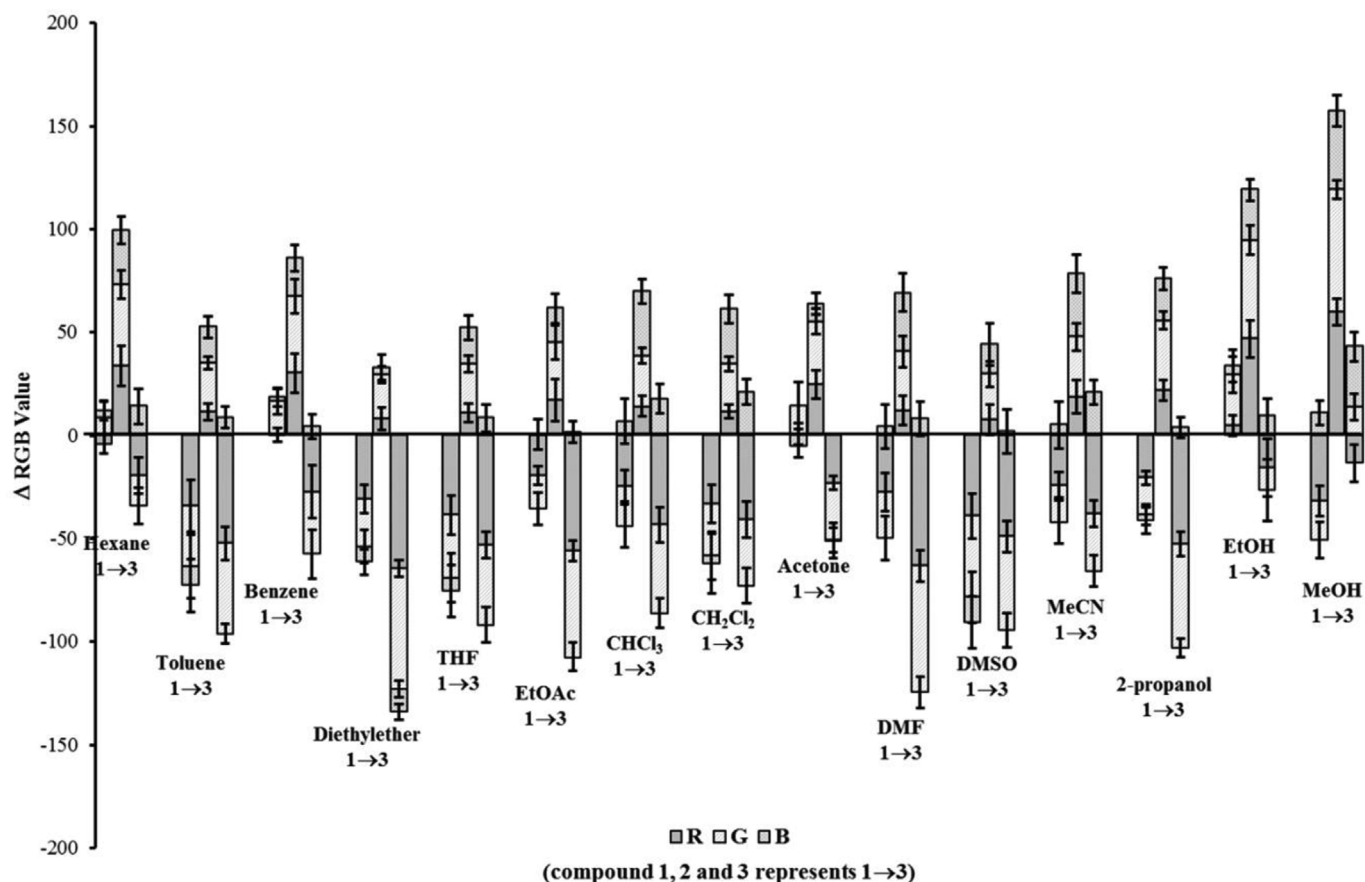


Fig. 4. Histogram plot of ΔRGB profile of a fluorometric paper-based sensor array of compounds 1, 2, and 3 after exposure to 15 saturated vapors of VOCs.

showed various color changes, as shown in Fig. 6. As the concentration of methanol increased, the emission intensity of compound 3 decreased. This result was attributed to the ESIPT process that was caused by hydrogen bonding of methanol.

4. Conclusion

A fluorometric paper based sensor array for detecting 15 different VOCs in the vapor phase with 100% accuracy has been successfully constructed by using salicylidene derivatives. Principle component analysis (PCA) of ΔRGB values obtained from images suggested that this novel fluorometric paper based sensor array has high reproducibility and

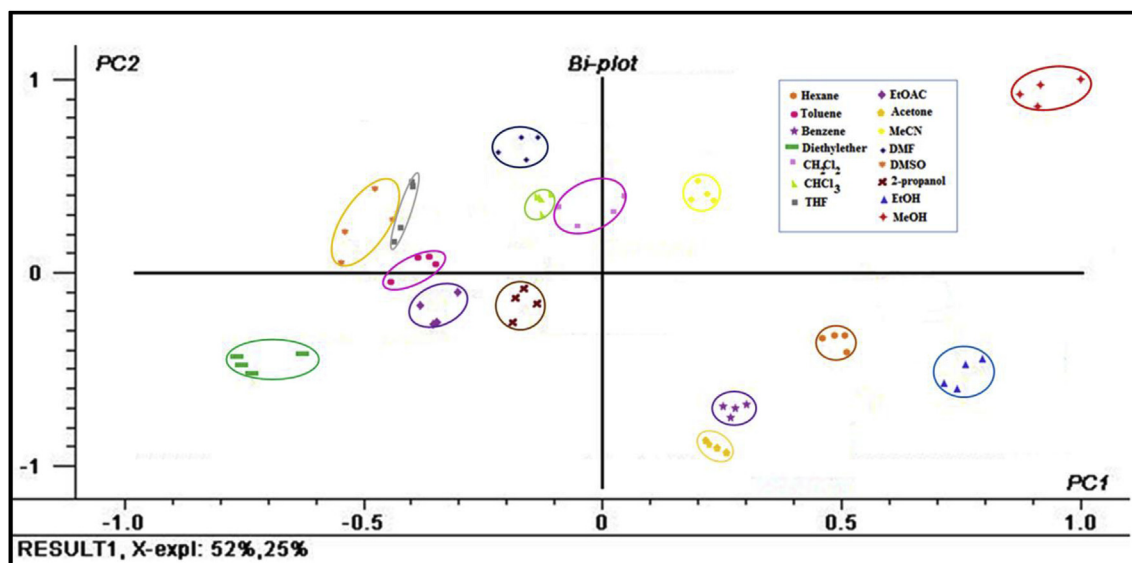


Fig. 5. PCA score plot of ΔRGB patterns of the images photographed from exposure of 15 VOC vapors onto fluorometric paper-based sensor arrays of compounds 1, 2, and 3 (3 sensor \times 15 VOCs \times 4 measurements).

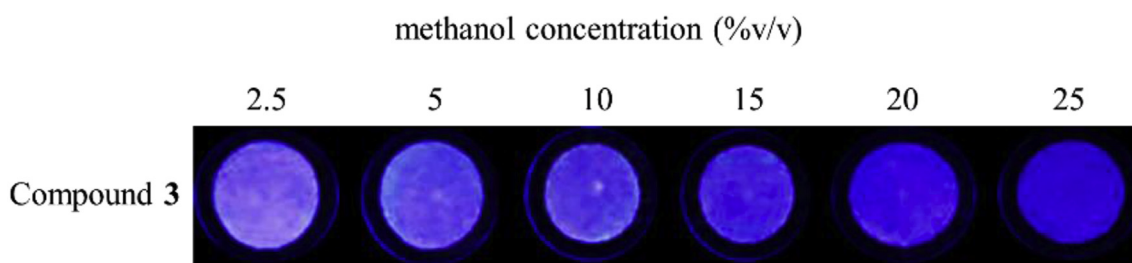


Fig. 6. Images illustrating the fluorescence responses of compound 3 paper based sensor array to various concentrations of methanol vapor in water.

discriminating ability towards 15 VOCs. Therefore, this portable fluorometric paper-based sensor array of salicylidene derivatives showed high potential in analyzing VOC vapors. In addition, compound 3 was also applicable to qualitatively determine the contamination of methanol in water. Thus, the salicylidene derivatives themselves should be valuable for the development of electronic tongue for VOC vapors related food analysis.

Acknowledgements

The authors gratefully thank the research fund for the Thailand Research Fund (MRG6180070). Master of Science would like to acknowledge the financial supports from Faculty of Science, the KMUTT 55th Anniversary Commemorative Fund. M.S. would also like to acknowledge the financial supports from National Nanotechnology Center (NANOTEC), NSTDA, Ministry of Science and Technology, Thailand, through its program of Center of Excellence Network.

Appendix A. Supplementary data

Supplementary data related to this article can be found at <http://dx.doi.org/10.1016/j.dyepig.2018.06.044>.

References

- [1] Phillips M, Herrera J, Krishnan S, Zain M, Greenberg J, Cataneo RN. *J Chromatogr B* 1999;729:75–88.
- [2] Tisser R, Young R. 6-The respiratory system. *Essential oil safety: a guide for health care professionals*. 2014. p. 99–110.
- [3] Natale CD, Macagnano A, Martinelli E, Paolesse R, D'Arcangelo G, Roscioni C, Finazzi-Agro A, D'Amico A. *Biosens Bioelectron* 2003;18:1209–18.
- [4] (a) Peng G, Trock E, Haick H. *Nano Lett* 2008;8:3631–5; (b) Chatterjee S, Castro M, Feller JF. *J Mater Chem B* 2013;36:4563–75.
- [5] (a) Lin H, Jang M, Suslick KS. *J Am Chem Soc* 2011;133:16786–9; (b) Chang Y, Tang N, Qu H, Liu J, Zhang D, Zhang H, Pang W, Duan X. *Sci Rep* 2016;6:23970–82; (c) Fair JD, Bailey WF, Felty RA, Gifford AE, Shultes B, Volles LH. *J Environ Sci* 2009;21:1005–8; (d) Maeda T, Onodera S, Ogino H. *J Chromatogr A* 1995;710:51–9.
- [6] Silva ML, Malcata FX. *J Enol Vitic* 1998;49:56–64.
- [7] (a) Vesely P, Jusk L, Basarova G, Seabrooks J, Ryder D. *J Agric Food Chem* 2003;51:6941–4; (b) Gerogiannaki-Christopoulou M. *J Food Technol* 2008;6:196–202.
- [8] (a) Lorwongtragool P, Sowade E, Watthanawisuth N, Baumann RR, Kerdcharoen T. *Sensors* 2014;14:19700–12; (b) Arshak K, Moore E, Lyons GM, Harris J, Clifford S. *Sens Rev* 2004;24:181–98.
- [9] (a) Ratnarathorn N, Chailapakul O, Henry CS, Dungchai W. *Talanta* 2012;99:552–7; (b) You GR, Jang HJ, Jo TG, Kim C. *RSC Adv* 2016;6:74400–8; (c) Lin Q, Chen P, Liu J, Fu YP, Zhang YM, Wei TB. *Dyes Pigments* 2013;98:100–5; (d) Wang S, Men G, Zhao L, Hou Q, Jiang S. *Binaphthyl-derived salicylidene Schiff base for dual-channel sensing of Cu, Zn cations and integrated molecular logic gates*. *Sensor Actuator B Chem* 2010;145:826–31; (e) Murale DP, Kim H, Choi WS, Churchill DG. *Highly selective excited state intramolecular proton transfer (ESIPT)-based superoxide probing*. *Org Lett* 2013;15:3946–9.
- [10] (a) Becuwe M, Landy D, Delattre F, Cazier F, Fourmentin S. *Fluorescent indolizine- β -cyclodextrin derivatives for the detection of volatile organic compounds*. *Sensors* 2008;8:3689–705; (b) Davis BW, Burris AJ, Niamnont N, Hare CD, Chen CY, Sukwattanasinitt M, Cheng Q. *Dual-mode optical sensing of organic vapors and proteins with polydiacetylene (PDA)-embedded electrospun nanofibers*. *Langmuir* 2014;30:9616–22; (c) Ji SM, Gwon SY, Kim SH. *Dyes Pigments* 2014;108:93–7; (d) Martini G, Martinelli E, Ruggeri G, Galli G, Pucci A. *Dyes Pigments*

- 2015;113:47–54; (e) Kim YJ, Gwon SY, Kim SH. *Dyes Pigments* 2016;133:184–8.
- [11] EC. Commission regulation 2870/2000 Laying down community reference methods for the analysis of sprits drinks. *Off J Eur Comm L* 2000;333:20–46.
- [12] (a) Yoon J, Chae SK, Kim JM. *Colorimetric sensors for volatile organic compounds (VOCs) based on conjugated polymer-embedded electrospun fibers*. *J Am Chem Soc* 2007;129:3038–9; (b) Suslick KS, Rakow NA, Sen A. *Colorimetric sensor arrays for molecular recognition*. *Tetrahedron Lett* 2004;60:11133–8; (c) Zhao W, Berg AVD. *Lab on paper*. *Lab Chip* 2008;8:1988–91; (d) Soga T, Jimbo Y, Suzuki K, Citterio D. *Inkjet-printed paper-based colorimetric sensor array for the discrimination of volatile primary amines*. *Anal Chem* 2013;85:8973–8; (e) Fraiwan A, Lee H, Choi S. *A paper-based cantilever array sensor: monitoring volatile organic compounds with naked eye*. *Talanta* 2016;158:57–62; (f) Zhu X, Zhang H, Wu J. *Chemiresistive ionogel sensor array for the detection and discrimination of volatile organic vapor*. *Sensor Actuator B Chem* 2014;202:105–13.
- [13] (a) Dolai S, Bhunia SK, Beglaryan SS, Kolusheva S, Zeiri L, Jelinek R. *Colorimetric polydiacetylene-aerogel detector for volatile organic compounds (VOCs)*. *Appl Mater Interface* 2017;9:2891–8; (b) Yoon B, Park IS, Shin H, Park HJ, Lee CW, Kim JM. *A litmus-type colorimetric and fluorometric volatile organic compound sensor based on inkjet-printed polydiacetylenes on paper substrates*. *Macromol Rapid Commun* 2013;34:731–5.
- [14] (a) Saravanakumar D, Devaraj S, Iyyampillai S, Mohandoss K, Kandaswamy M. *Schiff's base phenol-hydrazone derivatives as colorimetric chemosensors for fluoride ions*. *Tetrahedron Lett* 2008;49:127–32; (b) Li J, Lin H, Cai Z, Lin H. *A high selective anion colorimetric sensor based on salicylaldehyde for fluoride in aqueous media*. *Spectrochim Acta* 2009;72:1062–5; (c) Dalapati S, Alam MA, Jana S, Karmakar S, Guchhait N. "Test kit" for detection of biologically important anions: a salicylidene-hydrazine based Schiff base. *Spectrochim Acta* 2013;102:314–8; (d) Mukherjee S, Paul AK, Evans HS. *A family of highly selective fluorescent sensors for fluoride based on excited state proton transfer mechanism*. *Sensor Actuator B Chem* 2014;202:1190–9; (e) Zang L, Jiang S. *Substituent effects on anion sensing of salicylidene schiff base derivatives: tuning sensitivity and selectivity*. *Spectrochim Acta* 2015;150:814–20; (f) Erdemir S, Kocyyigit O. *Reversible "OFF-ON" fluorescent and colorimetric sensor based benzothiazole-bisphenol A for fluoride in MeCN*. *Sensor Actuator B Chem* 2015;221:900–5.
- [15] Fery-Forgues S, Lavabre D. *Are fluorescence quantum yields so tricky to measure? a demonstration using familiar stationary products*. *J Chem Educ* 1999;76:1260–4.
- [16] Eaidkong T, Mungkarnde R, Phollookin C, Tumcharern G, Sukwattanasinitt M, Wacharasindhu S. *Polydiacetylene paper based colorimetric sensor array for vapor phase detection and identification of volatile organic compounds*. *J Mater Chem* 2012;22:5970–7.
- [17] Surpateanu GG, Landy D, Lungu CN, Fourmentin S, Surpateanu G, Rethoreb C, Avarvari N. *Synthesis and inclusion capability of a β -cyclodextrin-tetrahydrovalene derivative*. *Tetrahedron Lett* 2006;62:9701–4.
- [18] AMc Cluskey, Robinson PJ, Hill T, Scottt JL, Edwards JK. *Green chemistry approaches to the Knoevenagel condensation: comparison of ethanol, water and solvent free (dry grind) approaches*. *Tetrahedron Lett* 2002;43:3117–20.
- [19] (a) Kotaka H, Konishi GI, Mizuno K. *Synthesis and photoluminescence properties of π -extended fluorine derivatives: the first example of a fluorescent solvatochromic nitro-group-containing dye with a high fluorescence quantum yield*. *Tetrahedron Lett* 2010;51:181–4; (b) Doroshenko AO, Posokhov EA, Verezubova AA, Ptyagina LM, Skripkina VT, Shershukov VM. *Radiationless deactivation of the excited phototautomer form and molecular structure of ES IPT-compounds*. *Photochem Photobiol Sci* 2002;1:92–9.
- [20] Sun W, Li S, Hu R, Qian Y, Wang S, Yang G. *Understanding solvent effects on luminescent properties of a triple fluorescent ES IPT compound and application for white light emission*. *J Phys Chem* 2009;113:5888–95.
- [21] Houjou H, Shingai H, Yagi K, Yoshikawa I, Araki K. *Mutual interference between intramolecular proton transfer sites through the adjoining π -conjugated system in schiff bases of double-headed, fused salicylaldehydes*. *J Org Chem* 2013;78:9021–31.
- [22] Ziolk M, Burdzinski G, Karolczak J. *Influence of intermolecular hydrogen bonding on the photochromic cycle of the aromatic schiff base *N,N'*-Bis(salicylidene)-*p*-phenylenediamine in Solution*. *J Phys Chem* 2009;113:2854–64.
- [23] Dalapati S, Alam MA, Jana S, Guchhait N. *Naked-eye detection of F⁻ and AcO⁻ ions by Schiff base receptor*. *J Fluorine Chem* 2011;132:536–40.
- [24] Hammami M, Rouissi H, Salah N, Selmi H, Otaibi MA, Blecker C, Karoui R. *Fluorescence spectroscopy coupled with factorial discriminant analysis technique to identify sheep milk from different feeding systems*. *Food Chem* 2010;122:1344–50.